

Cell-based mathematical models of electrophysiology

Karoline Horgmo Jæger & Aslak Tveito

[**simula** . research laboratory]

Contents

1. The membrane model (~1960s)
2. The bidomain model (~1970s)
3. The monodomain model (~1990s)
4. The Extracellular-Membrane-Intracellular (**EMI**) model (2017)
5. The Kirchhoff Network Model (**KNM**) (2023)
6. The Simplified Kirchhoff Network Model (**SKNM**) (2023)

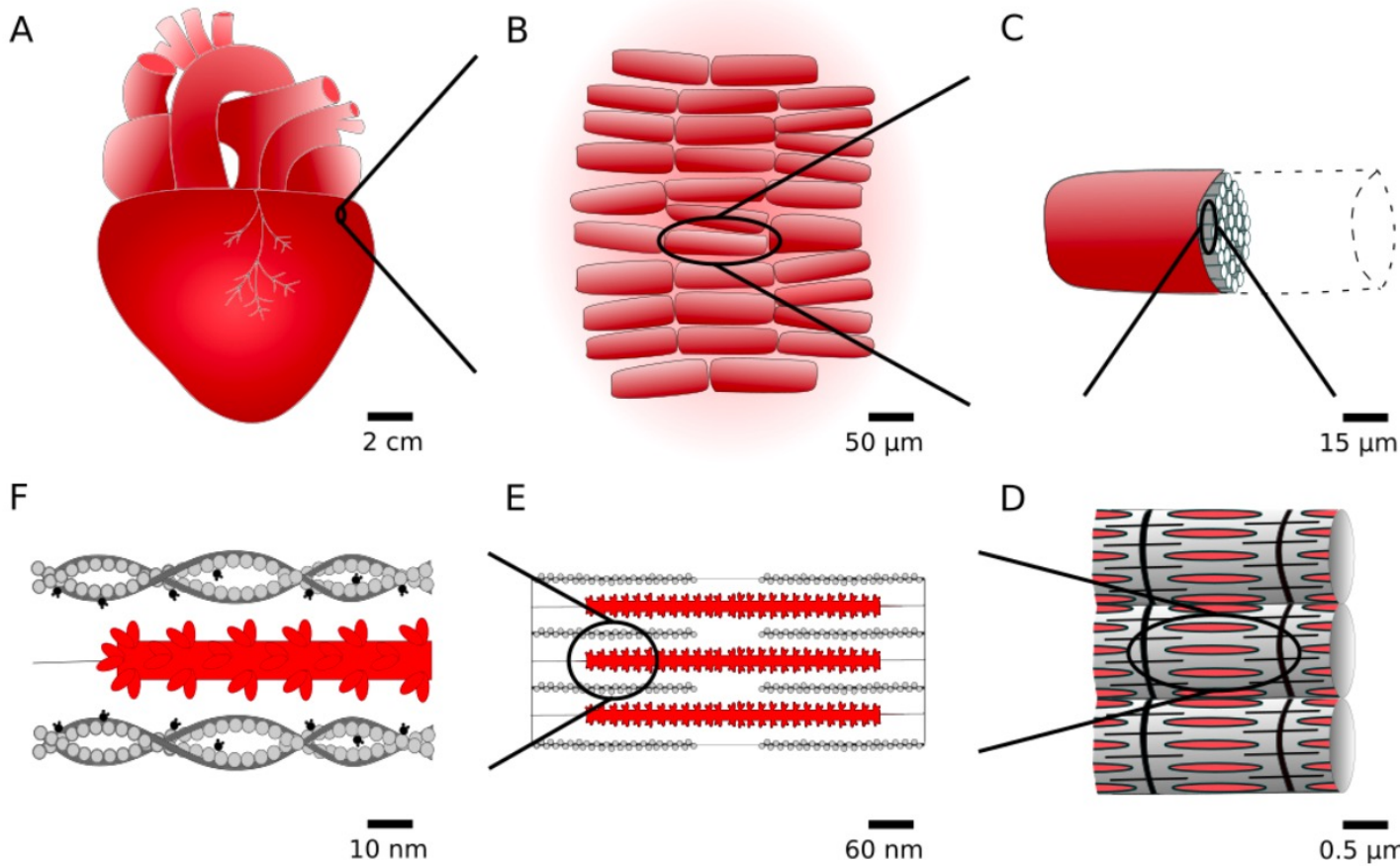


Figure I.2: Typical scales for mechanical modeling – from organ level to cross-bridges. The heart (A) is mainly composed of cardiac muscle cells, also called cardiomyocytes (B). Each cell (C) is composed of long tubes of sarcomeres (D), in which thin and thick myofilaments overlap in layers (E). The interaction between these (F) causes the cardiac muscle to contract in a process called the cross-bridge cycle. Figure from Paper [1].

Adult male heart
 \approx 300 g
 \approx 300 ml
 \approx Pumps about 7200 liters per day
 \approx 1900 gallons



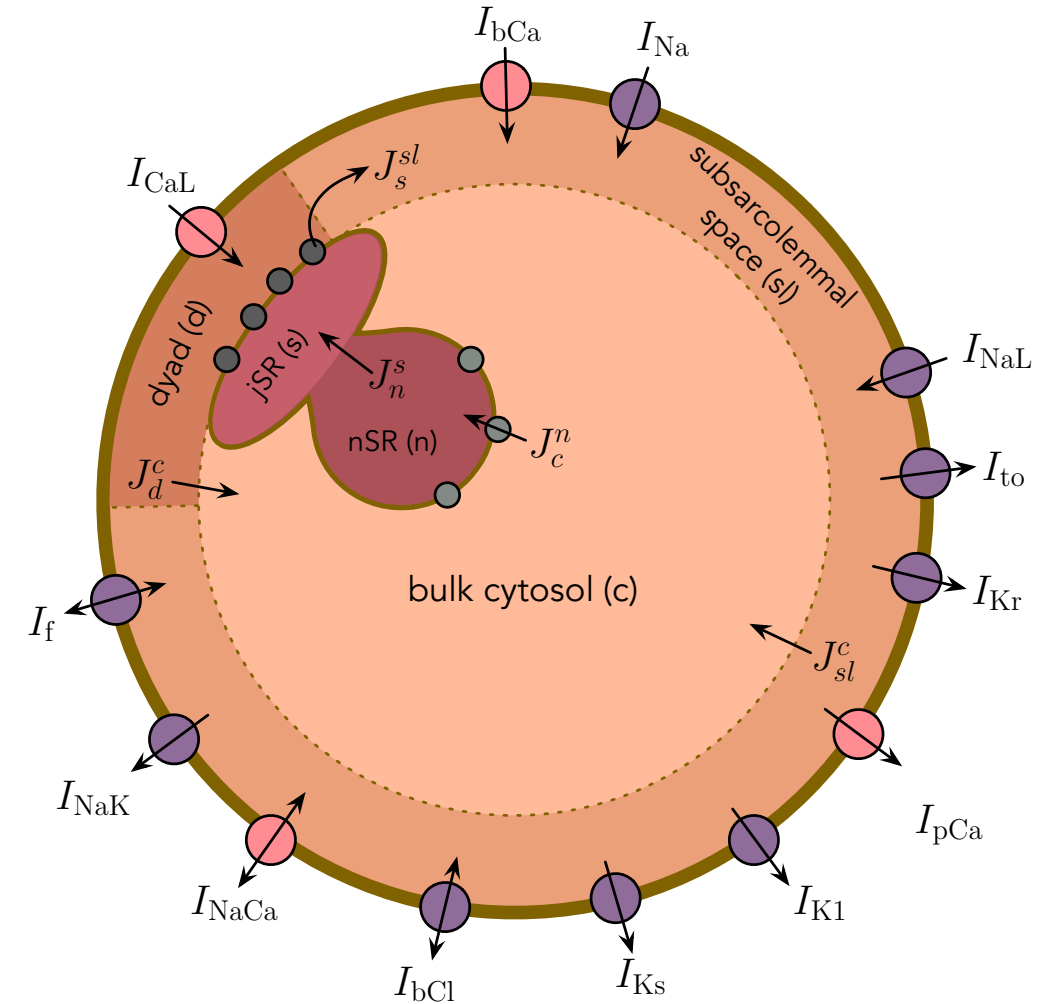
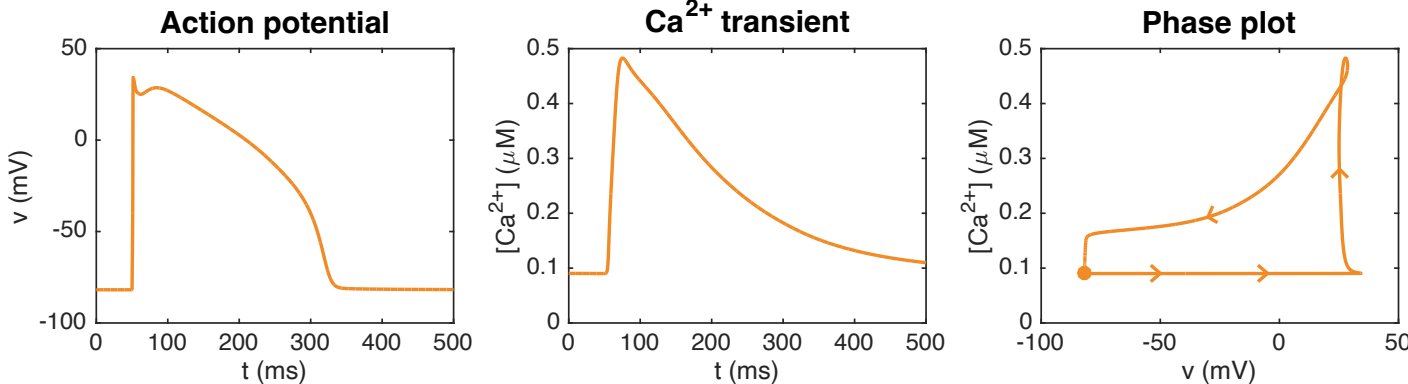
Scales of cardiac Electrophysiology
- Telle2023

Transmembrane potential & calcium transient

$$\frac{\partial v}{\partial t} = -\frac{1}{C_m} I_{\text{ion}}(v, s),$$

$$\frac{\partial s}{\partial t} = F(v, s)$$

v	membrane potential
s	additional state variables (e.g., channel gating and ionic concentrations)
t	time
C_m	membrane capacitance
I_{ion}	sum of current density through membrane proteins (e.g., ion channels)



There are several billion myocytes in the heart

Colossal modeling challenge

Classical models of cardiac tissue: homogenization, averaging

Assume that the extracellular space, the cell membrane, and the intracellular space exist everywhere

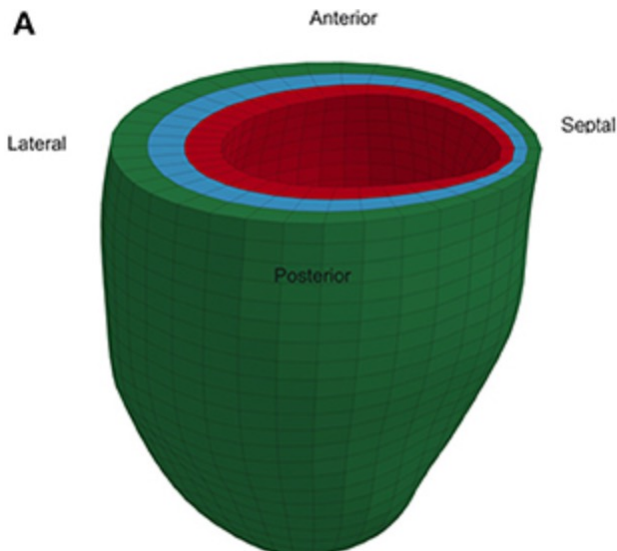
Removing the cell represents a dramatic simplification of the modeling

Monodomain model, Bidomain model

Modeling the tissue

Bidomain model

$$\begin{aligned}\chi C_m \left(\frac{\partial v}{\partial t} + I_{\text{ion}}(v, s) \right) &= \nabla \cdot (M_i \nabla v) + \nabla \cdot (M_i \nabla u_e), \\ 0 &= \nabla \cdot (M_i \nabla v) + \nabla \cdot ((M_i + M_e) \nabla u_e), \\ \frac{\partial s}{\partial t} &= F(v, s)\end{aligned}$$



Representative animal-specific
FE model of a rat LV.

Evaluation of a Novel Finite Element Model of Active Contraction in the Heart

Xiaoyan Zhang¹, Zhan-Qiu Liu¹, Kenneth S. Campbell² and Jonathan F. Wenk^{1,3*}

¹ Department of Mechanical Engineering, University of Kentucky, Lexington, KY, United States, ² Department of Physiology, University of Kentucky, Lexington, KY, United States, ³ Department of Surgery, University of Kentucky, Lexington, KY, United States

v	membrane potential
u _e	extracellular potential
s	additional state variables (e.g., channel gating and ionic concentrations)
t	time
C _m	membrane capacitance
I _{ion}	sum of current density through membrane proteins (e.g., ion channels)
χ	cell membrane surface to volume ratio
M _i	intracellular bidomain model conductivity
M _e	extracellular bidomain model conductivity

From bidomain to monodomain (from two voltages to one)

The bidomain model: $C_m \frac{\partial v}{\partial t} = \chi^{-1} (\nabla \cdot (M_i \nabla v) + \nabla \cdot (M_i \nabla u_e)) - I_{\text{ion}}(s, v),$
 $0 = \nabla \cdot (M_i \nabla v) + \nabla \cdot ((M_i + M_e) \nabla u_e),$

Assumption of equal anisotropy: $M_e = \lambda M_i$

Then:

$$\nabla \cdot (M_i \nabla u_e) = -\frac{1}{1+\lambda} \nabla \cdot (M_i \nabla v)$$

Therefore:

$$C_m \frac{\partial v}{\partial t} = \frac{\lambda}{\chi(1+\lambda)} \nabla \cdot (M_i \nabla v) - I_{\text{ion}}(s, v),$$
$$\frac{ds}{dt} = F(s, v).$$

which is the monodomain model

Monodomain model (assume $M_e = \lambda M_i$)

$$\begin{aligned} \chi C_m \left(\frac{\partial v}{\partial t} + I_{\text{ion}}(v, s) \right) &= \frac{\lambda}{1 + \lambda} \nabla \cdot (M_i \nabla v), \\ \frac{\partial s}{\partial t} &= F(v, s) \end{aligned}$$

v	membrane potential
u_e	extracellular potential
s	additional state variables (e.g., channel gating and ionic concentrations)
t	time
C_m	membrane capacitance
I_{ion}	sum of current density through membrane proteins (e.g., ion channels)
χ	cell membrane surface to volume ratio
M_i	intracellular bidomain model conductivity

Bidomain and monodomain example

2D sheet of hiPSC-CMs (human induced pluripotent stem cell-derived cardiomyocytes)

M _e	4 mS/cm
M _i	0 - 3.2 mS/cm (random variation)



Because M_e is constant and M_i varies, the assumption $M_e = \lambda M_i$ cannot hold

We approximate λ by minimizing $F(\lambda) = \frac{1}{2} \int_{\Omega} ((M_e^x - \lambda M_i^x)^2 + (M_e^y - \lambda M_i^y)^2) dS$

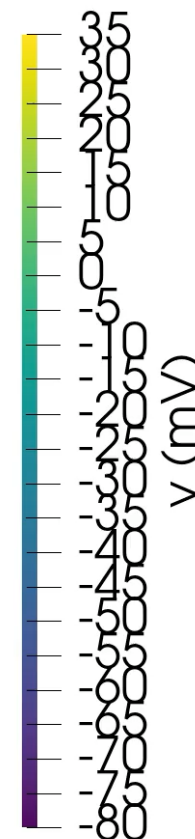
The optimal λ is then given by $\lambda = \frac{\int_{\Omega} M_e^x M_i^x dS + \int_{\Omega} M_e^y M_i^y dS}{\int_{\Omega} (M_i^x)^2 dS + \int_{\Omega} (M_i^y)^2 dS}$

$T = 1 \text{ ms}$

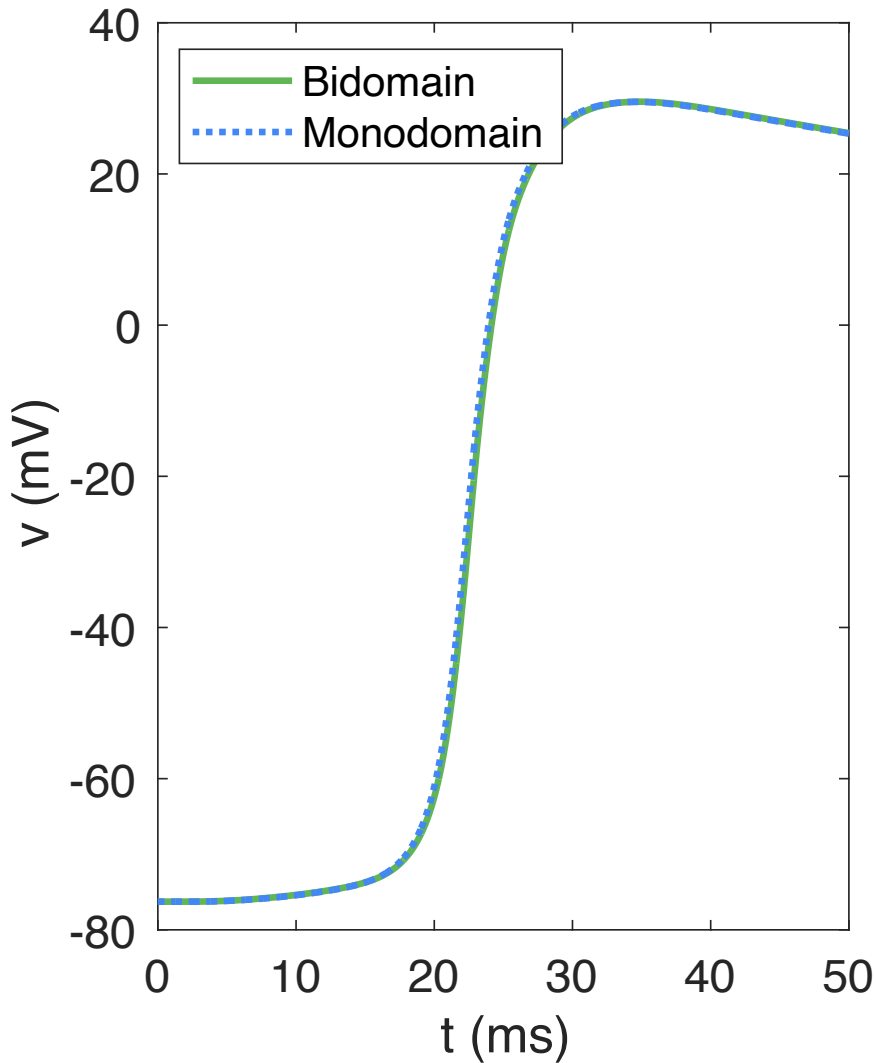
Bidomain



Monodomain



Comparison of solution in
the center of the domain:



Comparison of CPU time:

Model	CPU time
Bidomain	18 min
Monodomain	1.5 min

Applications of the bidomain/monodomain models

Understanding and Predicting Cardiac Arrhythmias

1. Simulates mechanisms underlying arrhythmias
2. Models re-entrant circuits causing tachycardia

Drug Development and Testing

1. Predicts effects of cellular changes (e.g., ion channel blocking) on the whole heart
2. Valuable for testing new cardiac drugs

Cardiac Device Design and Testing

1. Useful for design and testing of devices like pacemakers and defibrillators
2. Helps understand how electric currents from devices spread through heart tissue

Understanding Cardiac Ischemia

1. Models changes in cardiac tissue during ischemia
2. Helps understand how ischemia alters the heart's electrical conduction



Computational Physiology

Simula Summer School 2021 – Student Reports

simula

OPEN ACCESS

 Springer



Chapter 2

3D Simulations of Fetal and Maternal Ventricular Excitation for Investigating the Abdominal ECG

Julie Johanne Uv¹, Lena Myklebust¹, Hamid Khoshfekr Rudsari^{2,3}, Hannes Welle⁴, Hermenegild Arevalo¹

1 – Simula Research Laboratory, Norway

2 – University of Oslo, Norway

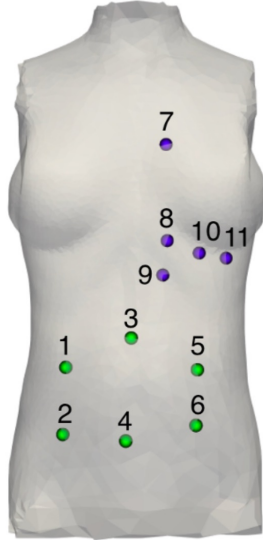
3 – Oslo University Hospital, Norway

4 – Karlsruhe Institute of Technology, Germany

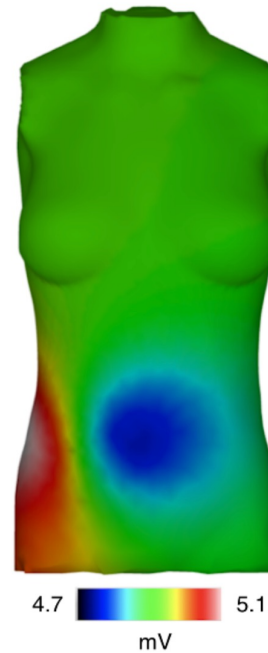
Abstract Congenital heart disease (CHD) is a leading cause of infant death. To diagnose CHD, recordings from abdominal fetal electrocardiograms (fECG) can be used as a non-invasive tool. However, it is challenging to extract the fetal signal from fECG recordings partly due to the lack of data combining fECG recordings with a ground truth for the fetal signal, which can be obtained by using a scalp electrode during delivery. In this study, we present a computational model of a pregnant



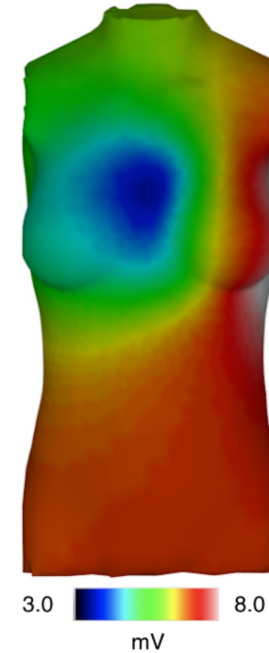
(a) Visualisation of the finite element mesh used in our simulations. Hearts and torso are based on models by [21] and the FEMONUM database [24, 25, 26] respectively.



(b) The extracellular potential was measured at 11 nodes on the torso to obtain fECG traces. The figure shows thoracic (purple) and abdominal (green) electrodes. Numbers denote the different channels used for signal processing.



4.7 5.1
mV



3.0 8.0
mV

Fig. 2.4: Extracellular potential on the torso surface 5 ms after stimulation of the fetal (left) and maternal heart (right).

The bidomain/monodomain models are available in well-tested software.

Both have been used for a large variety of applications and have provided reasonable results for tissue level simulations.

What is missing in the homogenized (bidomain/monodomain) models?

What is missing in the homogenized (bidomain/monodomain) models?

The Cell!

The **extracellular** space, the **cell membrane** and the
intracellular space are assumed to exist

Everywhere

Challenges for the averaged models

1. The cell is missing in the bidomain/monodomain models
2. Typical bidomain computational mesh size is $\Delta x \approx 0.25\text{mm}$, thus one mesh block contains about $(0.25\text{mm})^3 / 16\text{pL} \approx 1000$ myocytes (depending on cell type)
3. Mesh refinement does not recreate the cell – it is averaged away forever
4. In bidomain/monodomain models there is no way to represent properties that vary along the cell, or differences from cell to cell
5. Bidomain/monodomain models are suitable for mm-considerations – but not for μm considerations

Modeling by homogenization/averaging

Heat equation

Represents averaging over an enormous number of molecules or atoms

Atomic radius of a metal is typically around 0.1 nm

Macro scale for a metal rod (say 1 cm) is about 10^8 times larger than the micro scale

Bidomain and monodomain models

Length of a ventricular cardiomyocyte is about 100 μm

Interested in phenomena at the mm/cm-scale

Micro scale is only 10-100 times smaller than the macro scale

Cell-based model of electrophysiology

The objective is to develop a model that represents each individual cell.

The model should allow ion channel density to vary along the cell membrane.

It should allow the degree of coupling between individual myocytes to vary from one coupling to another.

The model is required to have sub-cell resolution.

The computational mesh of the model must be at the micrometer (μm) scale.

This high-resolution model will facilitate the investigation of electrophysiology dynamics near individual cardiomyocytes.

The EMI model

Extracellular, Membrane, Intracellular

The EMI model for one cell

$$\nabla \cdot \sigma_i \nabla u_i = 0, \text{ in } \Omega_i,$$

$$\nabla \cdot \sigma_e \nabla u_e = 0, \text{ in } \Omega_e,$$

$$u_e = 0, \text{ at } \partial\Omega_e^D,$$

$$\mathbf{n}_e \cdot \sigma_e \nabla u_e = 0, \text{ at } \partial\Omega_e^N,$$

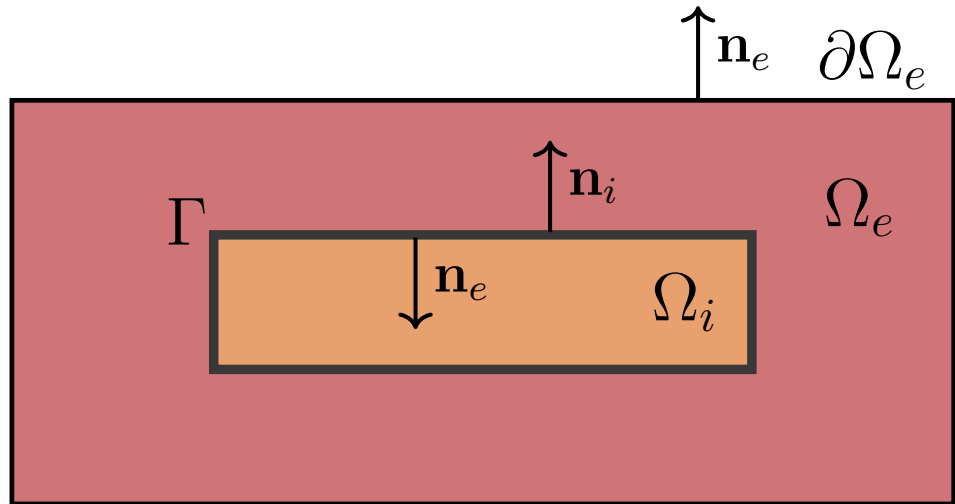
$$\mathbf{n}_e \cdot \sigma_e \nabla u_e = -\mathbf{n}_i \cdot \sigma_i \nabla u_i, \text{ at } \Gamma,$$

$$u_i - u_e = v, \text{ at } \Gamma,$$

$$I_m = -\mathbf{n}_i \cdot \sigma_i \nabla u_i, \text{ at } \Gamma,$$

$$\frac{\partial v}{\partial t} = \frac{1}{C_m} (I_m - I_{\text{ion}}), \text{ at } \Gamma,$$

$$\frac{\partial s}{\partial t} = F(v, s), \text{ at } \Gamma,$$



v	membrane potential
u _i	intracellular potential
u _e	extracellular potential
s	additional state variables (e.g., channel gating and ionic concentrations)
t	time
C _m	membrane capacitance
I _{ion}	sum of current density through membrane proteins
σ _i	intracellular conductivity
σ _e	extracellular conductivity

EMI for two cells connected by gap junctions

$$\nabla \cdot \sigma_i \nabla u_i^k = 0 \quad \text{in } \Omega_i^k,$$

$$\nabla \cdot \sigma_e \nabla u_e = 0 \quad \text{in } \Omega_e,$$

$$u_e = 0 \quad \text{at } \partial\Omega_e^D,$$

$$n_e \cdot \sigma_e \nabla u_e = 0 \quad \text{at } \partial\Omega_e^N,$$

$$u_i^k - u_e = v^k \quad \text{at } \Gamma_k,$$

$$s_t^k = F^k \quad \text{at } \Gamma_k,$$

$$n_e \cdot \sigma_e \nabla u_e = -n_i^k \cdot \sigma_i \nabla u_i^k \equiv I_m^k \quad \text{at } \Gamma_k,$$

$$v_t^k = \frac{1}{C_m} (I_m^k - I_{\text{ion}}^k) \quad \text{at } \Gamma_k,$$

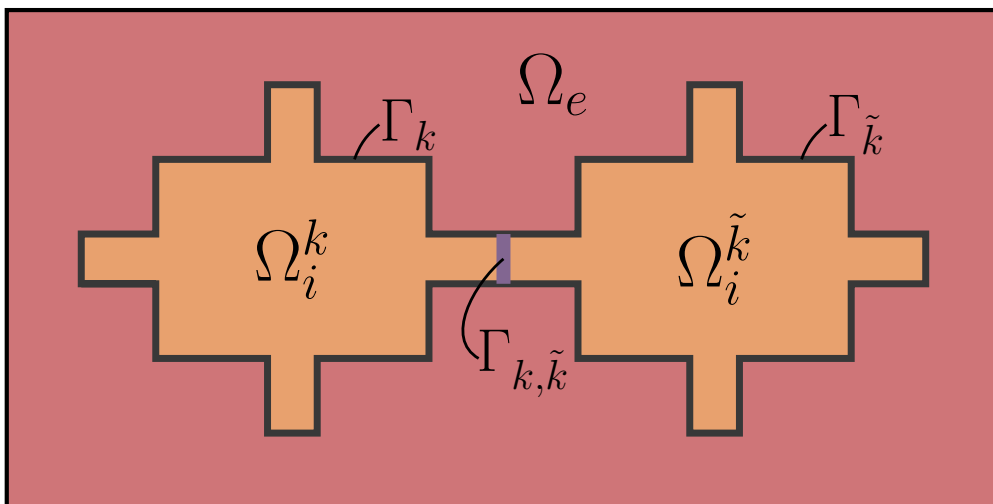
$$u_i^k - u_{\tilde{k}}^{\tilde{k}} = w^k \quad \text{at } \Gamma_{k,\tilde{k}},$$

$$n_i^{\tilde{k}} \cdot \sigma_i \nabla u_i^{\tilde{k}} = -n_i^k \cdot \sigma_i \nabla u_i^k \equiv I_{k,\tilde{k}} \quad \text{at } \Gamma_{k,\tilde{k}},$$

$$w_t^k = \frac{1}{C_g} (I_{k,\tilde{k}} - I_{\text{gap}}^k) \quad \text{at } \Gamma_{k,\tilde{k}},$$

for each cell k and each neighboring cell \tilde{k} .

Note that all **EMI** simulations are in **3D** (or else the extracellular space would not be connected)



v	membrane potential
u_i	intracellular potential
u_e	extracellular potential
s	additional state variables (e.g., channel gating and ionic concentrations)
t	time
C_m	membrane capacitance
C_g	intercalated disc capacitance
I_{ion}	sum of current density through membrane proteins (e.g., ion channels)
I_{gap}	sum of current density through gap junctions between neighbouring cells
σ_i	intracellular conductivity
σ_e	extracellular conductivity

Fig 2. Cell geometry used in the simulations.

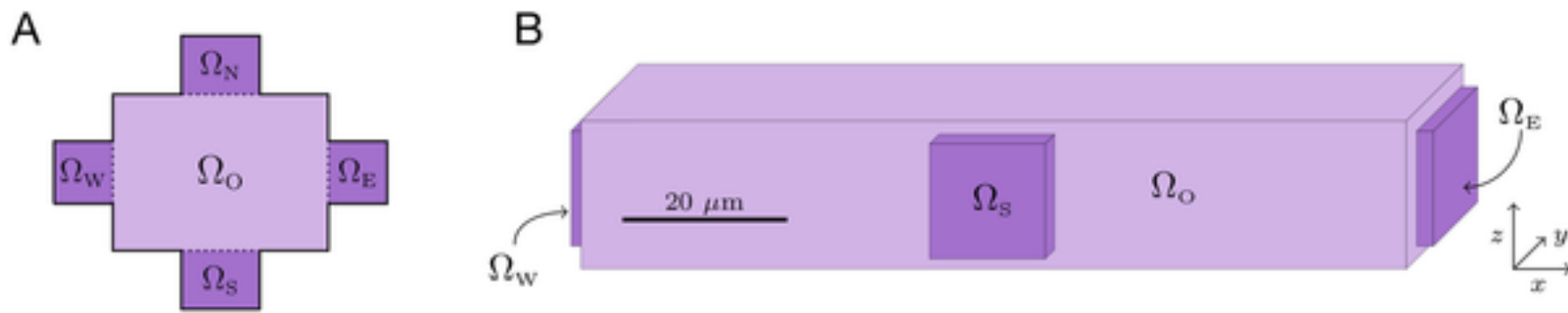
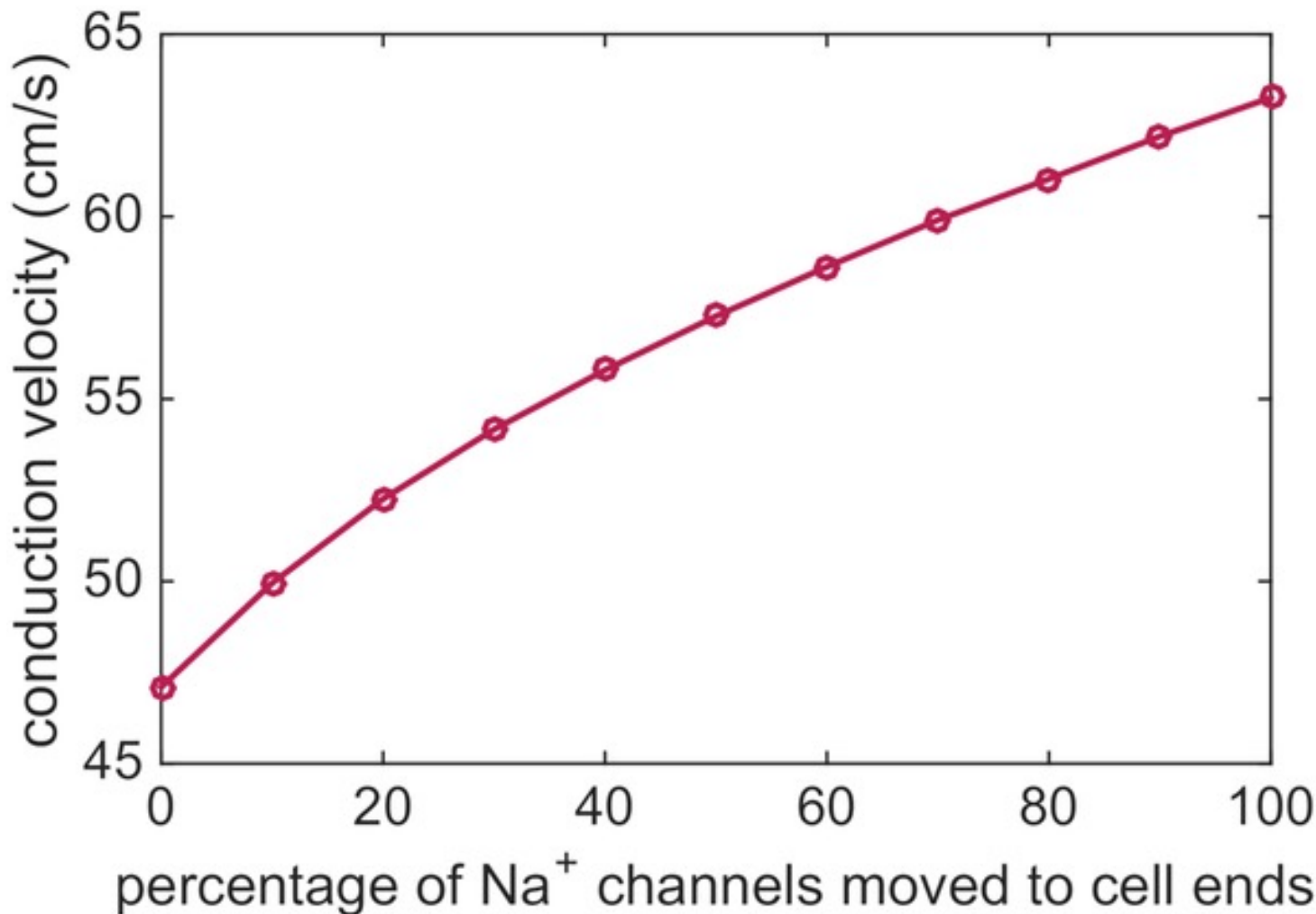
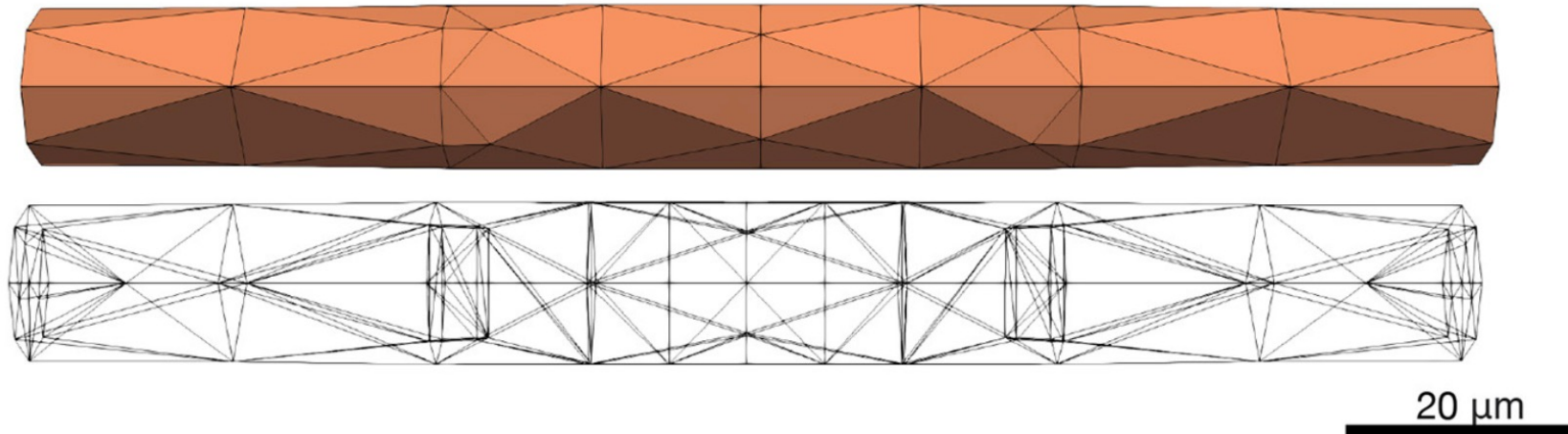


Fig 4. The conduction velocity increases as a larger percentage of the sodium channels is moved to the cell ends.



A Approximate single myocyte morphology and computational mesh



B EMI model domain for four connected myocytes (3D)

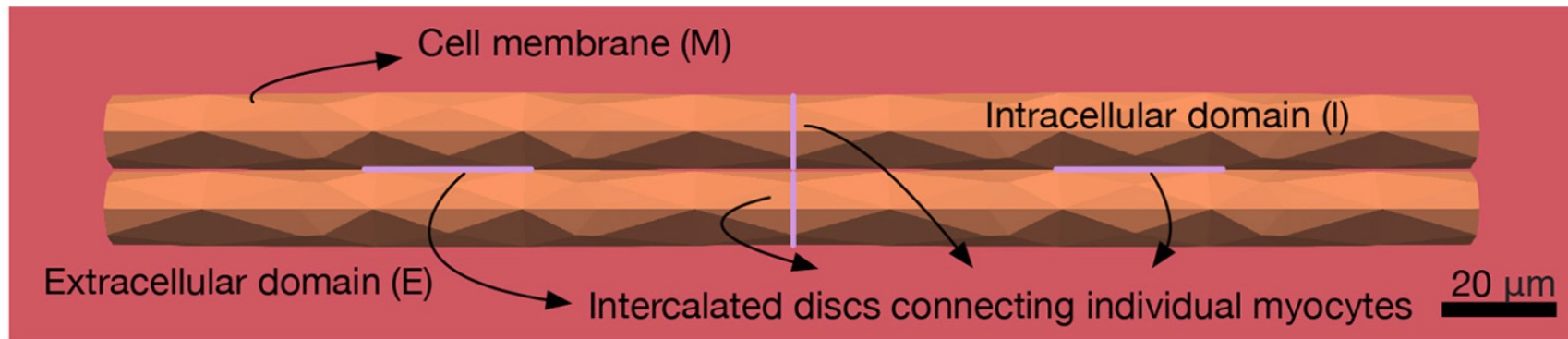


FIGURE 1 | Illustration of the EMI model domain. **(A)** Shows the approximate cylindrical geometry and associated mesh of a single myocyte of length 120 μm and diameter ranging from 13 to 14 μm (Nygren et al., 1998). **(B)** Shows an illustration of the different components of the EMI model domain for an example collection of four connected myocytes. The domain consists of a number of myocytes surrounded by an extracellular space. The cell membrane is defined at the interface between the intracellular and extracellular spaces and intercalated discs with gap junctions are defined at the interface between adjacent myocytes. All computations presented here are in 3D.

EMI model application

- The outlet of the pulmonary vein is a known initiation site for atrial fibrillation
- A number of mutations are known to increase the risk of atrial fibrillation, e.g., the N588K I_{Kr} gain of function mutation
- EMI model simulation of a mix of pulmonary vein and left atrial cardiomyocytes with spatially varying cell coupling (next slide):
 - re-entry for the N588K mutation
 - no re-entry for the wild type case

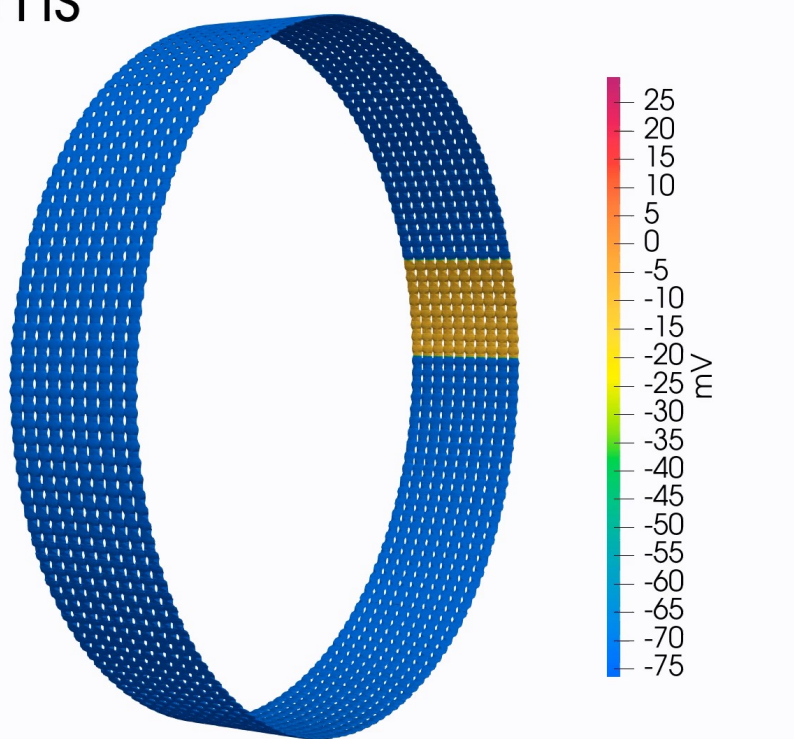
Arrhythmogenic influence
of mutations in a myocyte-based
computational model
of the pulmonary vein sleeve

Karoline Horgmo Jæger¹, Andrew G. Edwards¹, Wayne R. Giles^{1,2} & Aslak Tveito¹

EMI model simulations of the outlet of a pulmonary vein

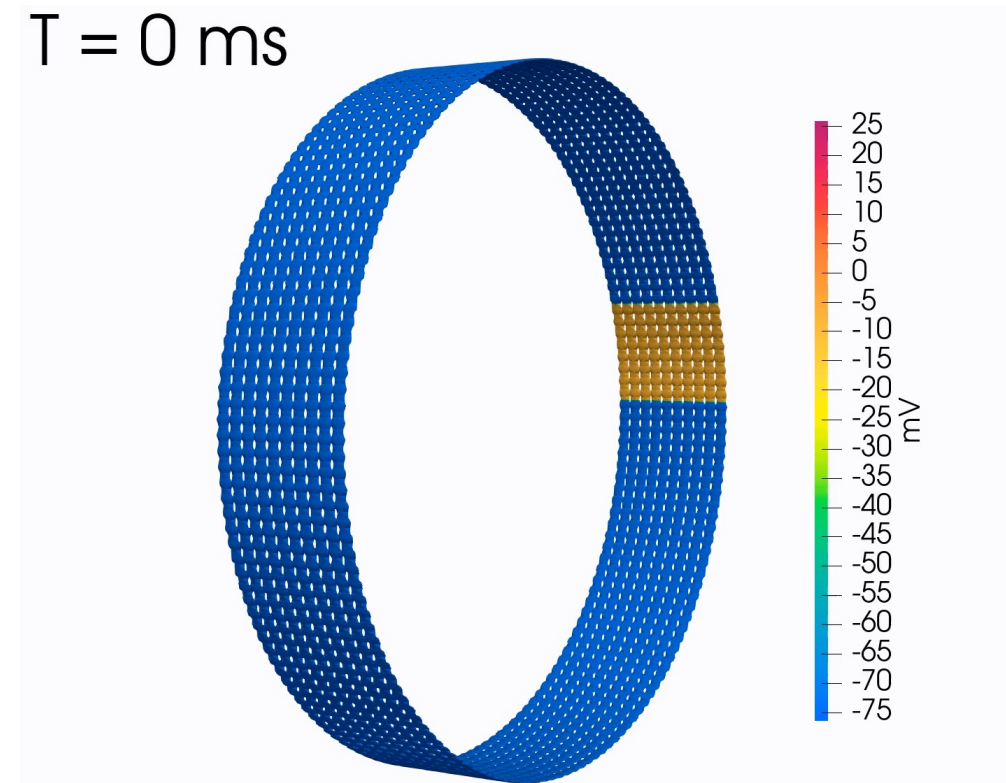
Wild type case: no re-entry

T = 0 ms



N588K mutation: re-entry

T = 0 ms



The human heart:

- state of the art for the bidomain model
- out of reach for EMI

Rough estimates:

Volume of one myocyte (+extracellular space)	30 pL (see [1,2])
Total volume	300 mL (see [7])
Number of cardiac cells (not only myocytes)	$300 \text{ mL}/30 \text{ pL} = 10 \times 10^9$
Resolved resolution bidomain	$\Delta x = 0.25 \text{ mm}$ (see [3,4,5,6])
Resolved resolution EMI	$\Delta x = 10 \mu\text{m}$
#mesh points bidomain	19.2×10^6
#mesh points EMI	300×10^9

Applicability of the EMI approach

Well suited for small collections of cells (~ 1000)

Possible to study whole hearts of small animals

Possible to study AV-node, SA-node, etc.

Possible to study special parts of the heart, for example:

- Outlet of pulmonary veins
- Vicinity of ischemic regions
- Effect of scar tissue

Not suited for whole heart simulations of humans or large animals

State of modeling

Bidomain/monodomain

Computationally feasible but too coarse at the cellular level

EMI

Computationally very demanding but also very accurate

State of modeling

Bidomain/monodomain

Computationally feasible but too coarse at the cellular level

EMI

Computationally very demanding but also very accurate

Question

Can we find something in between;
computationally feasible and accurate at the cell level?

Efficient, cell-based simulations of cardiac electrophysiology; The Kirchhoff Network Model (KNM)

Karoline Horgmo Jæger¹ and Aslak Tveito¹

¹Simula Research Laboratory, Norway

March 16, 2023

Model based on representation of individual cells and surrounding extracellular compartments

Cell-level accuracy, but not sub-cellular

Much faster than EMI and faster than bidomain

KNM is similar to the bidomain model
SKNM is similar to the monodomain model

Cell-level accuracy

Very fast method

The Simplified Kirchhoff Network Model (SKNM); a cell-based reaction-diffusion model of excitable tissue

Karoline Horgmo Jæger¹ and Aslak Tveito¹

¹Simula Research Laboratory, Norway

May 16, 2023

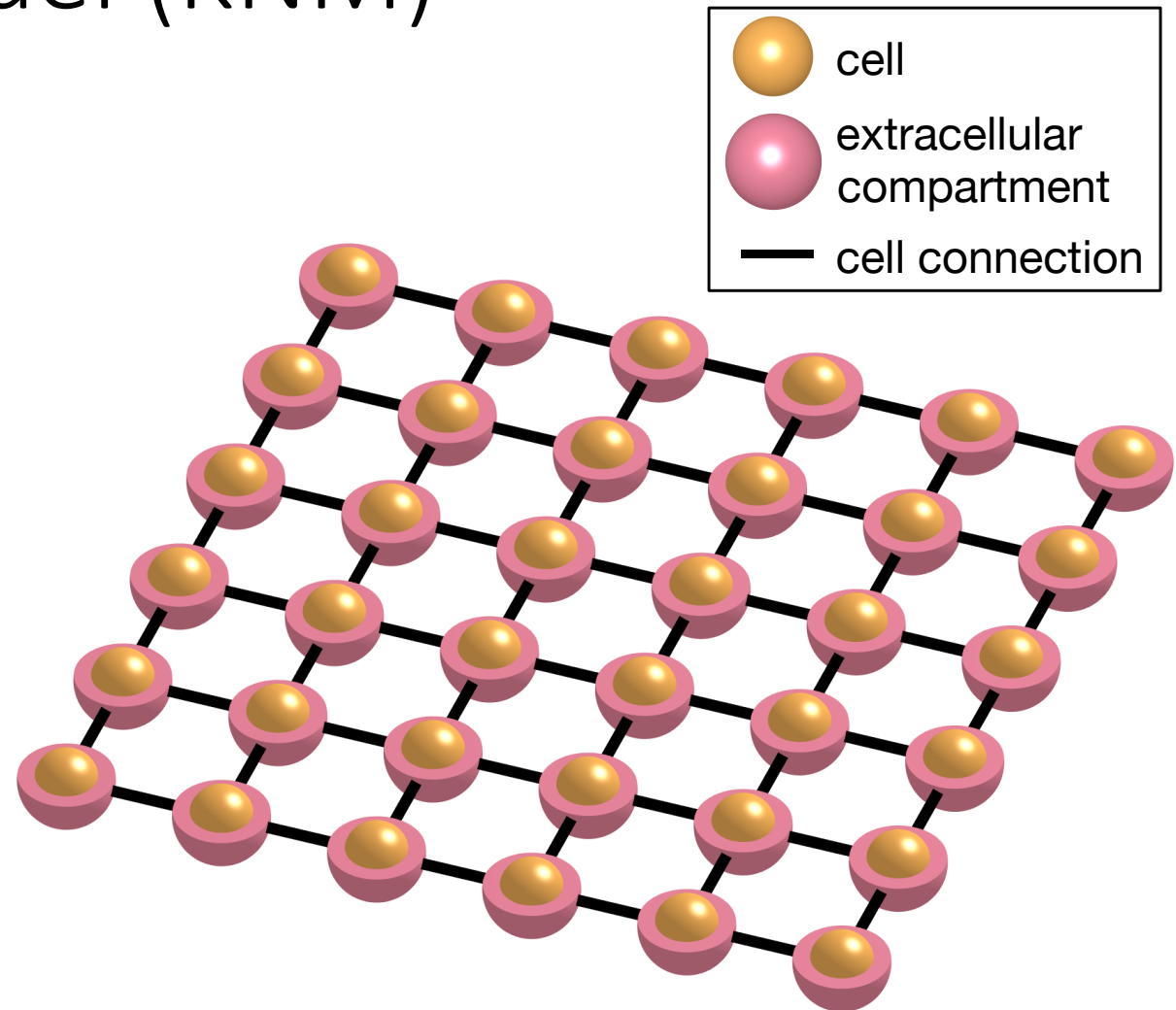
Kirchhoff Network Model (KNM)

Kirchhoff's current law:

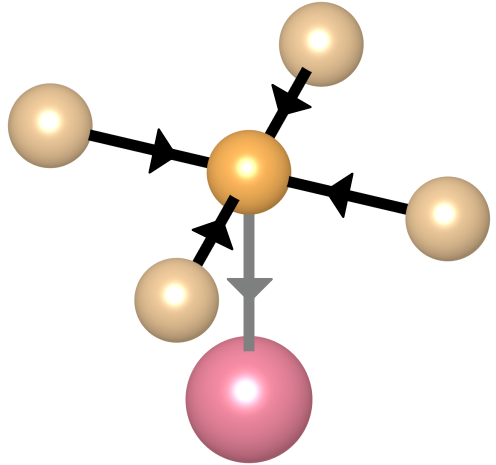
The sum of currents into a node must equal the sum of currents out of the node

Kirchhoff Network Model:

Let each cell and a surrounding extracellular compartment be the nodes, and apply Kirchhoff's current law for each node



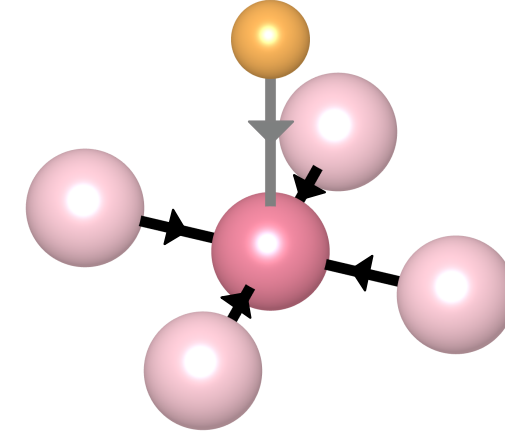
Kirchhoff's current law: The sum of currents into a node must equal the sum of currents out of the node



cell k
neighboring cells $j \in N_k$
extracellular compartment k
— cell connection, $I_i^{j,k}$
— cell membrane, I_m^k

Kirchhoff's current law applied for **each cell, k :**

$$I_m^k = \sum_{j \in N_k} I_i^{j,k} \quad (1)$$



cell k
extracellular compartment k
neighboring extracellular compartment $j \in N_k$
— extracellular connection, $I_e^{j,k}$
— cell membrane, I_m^k

Kirchhoff's current law applied for **each extracellular compartment, k :**

$$I_m^k + \sum_{j \in N_k} I_e^{j,k} = 0 \quad (2)$$

(1) inserted in (2) gives:

$$\sum_{j \in N_k} I_i^{j,k} + \sum_{j \in N_k} I_e^{j,k} = 0 \quad (3)$$

$$\text{Here, } I_i^{j,k} = G_i^{j,k}(u_i^j - u_i^k) \quad (4)$$

$$I_e^{j,k} = G_e^{j,k}(u_e^j - u_e^k) \quad (5)$$

$$I_m^k = A_m^k \left(C_m \frac{dv^k}{dt} + I_{\text{ion}}^k(v^k, s^k) \right) \quad (6)$$

$$v^k = u_i^k - u_e^k \quad (7)$$

KNM is (4)–(7)
inserted in (1)
and (3)

Kirchhoff Network Model (KNM)

For each cell, k:

$$C_m \frac{dv^k}{dt} = \frac{1}{A_m^k} \sum_{j \in N_k} \{ G_i^{j,k} (v^j - v^k) + G_e^{j,k} (u_e^j - u_e^k) \} - I_{\text{ion}}^k (v^k, s^k),$$

$$0 = \sum_{j \in N_k} G_i^{j,k} (v^j - v^k) + \sum_{j \in N_k} (G_i^{j,k} + G_e^{j,k}) (u_e^j - u_e^k)$$

$$\frac{ds^k}{dt} = F_k(s^k, v^k),$$

where N_k are the neighboring cells of cell k

v_k	membrane potential of cell k
u_e^k	extracellular potential of extracellular compartment surrounding cell k
s^k	additional state variables for cell k (e.g., channel gating and ionic concentrations)
t	time
C_m	membrane capacitance
I_{ion}^k	sum of current density through membrane proteins (e.g., ion channels) of cell k
A_m^k	cell membrane surface area
$G_i^{j,k}$	intracellular conductance between cell k and neighboring cell j
$G_e^{j,k}$	extracellular conductance between the extracellular compartments associated with cells k and j

Simplified Kirchhoff Network Model (SKNM)

SKNM can be derived from KNM like the monodomain model is derived from the bidomain model

1) KNM: $C_m \frac{dv^k}{dt} = \frac{1}{A_m^k} \sum_{j \in N_k} \{G_i^{j,k}(v^j - v^k) + G_e^{j,k}(u_e^j - u_e^k)\} - I_{\text{ion}}^k(v^k, s^k),$

$$0 = \sum_{j \in N_k} G_i^{j,k} (v^j - v^k) + \sum_{j \in N_k} (G_i^{j,k} + G_e^{j,k})(u_e^j - u_e^k)$$

2) Assume: $G_e^{j,k} = \lambda G_i^{j,k}$

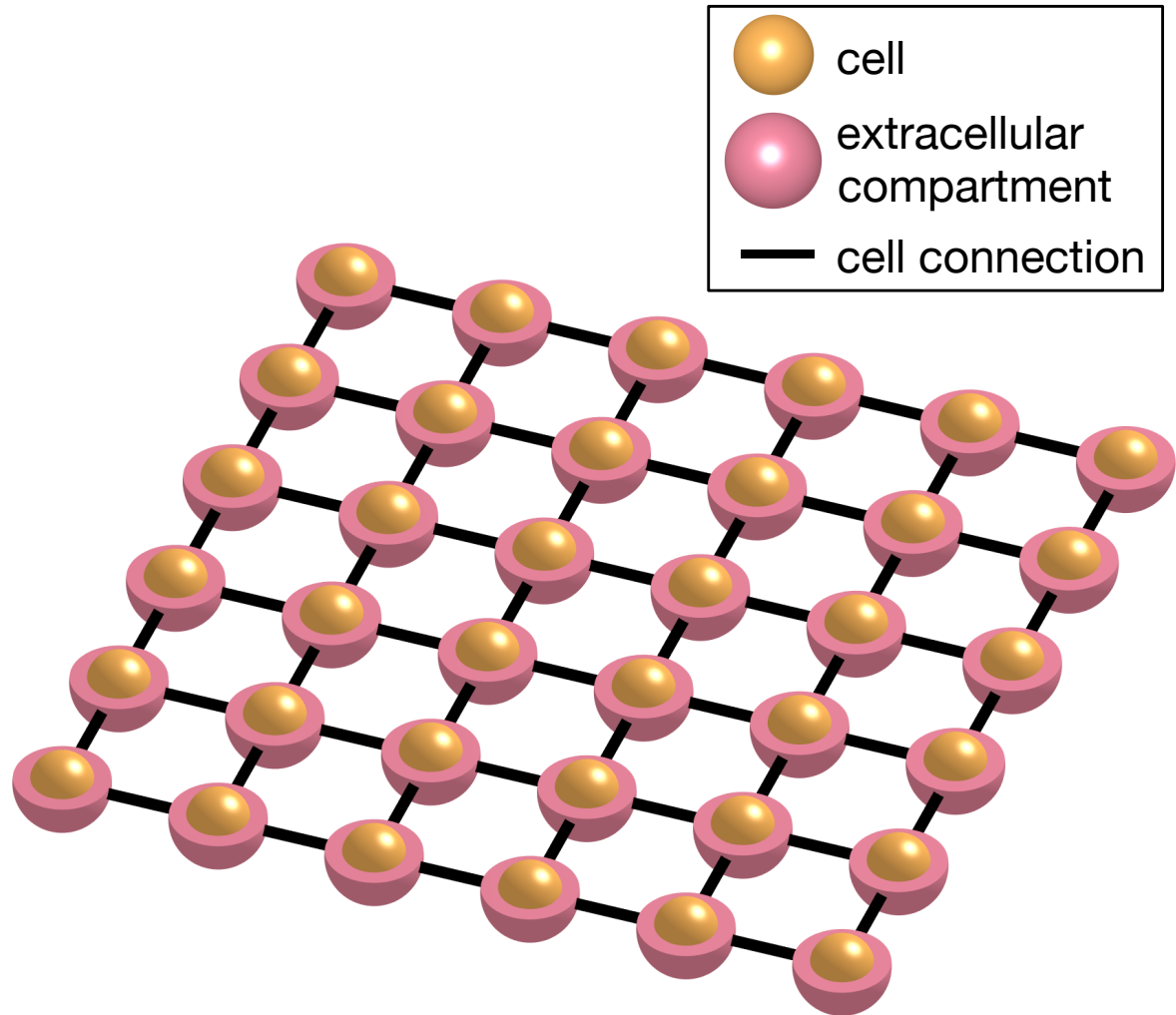
3) Then: $\sum_{j \in N_k} G_i^{j,k}(u_e^j - u_e^k) = -\frac{1}{1 + \lambda} \sum_{j \in N_k} G_i^{j,k} (v^j - v^k)$

4) Therefore: $C_m \frac{dv^k}{dt} = \frac{\lambda}{A_m^k(1 + \lambda)} \sum_{j \in N_k} G_i^{j,k}(v^j - v^k) - I_{\text{ion}}^k(v^k, s^k)$

which is SKNM

KNM/SKNM model components:

- 1) Membrane capacitance (C_m) and membrane area of each cell (A_m^k)
- 2) Model for the membrane dynamics (I_{ion}^k, F_k)
- 3) Overview of cell connections (N_j)
- 4) Strength of cell connections ($G_i^{j,k}$)
- 5) Strength of extracellular connections ($G_e^{j,k}$)

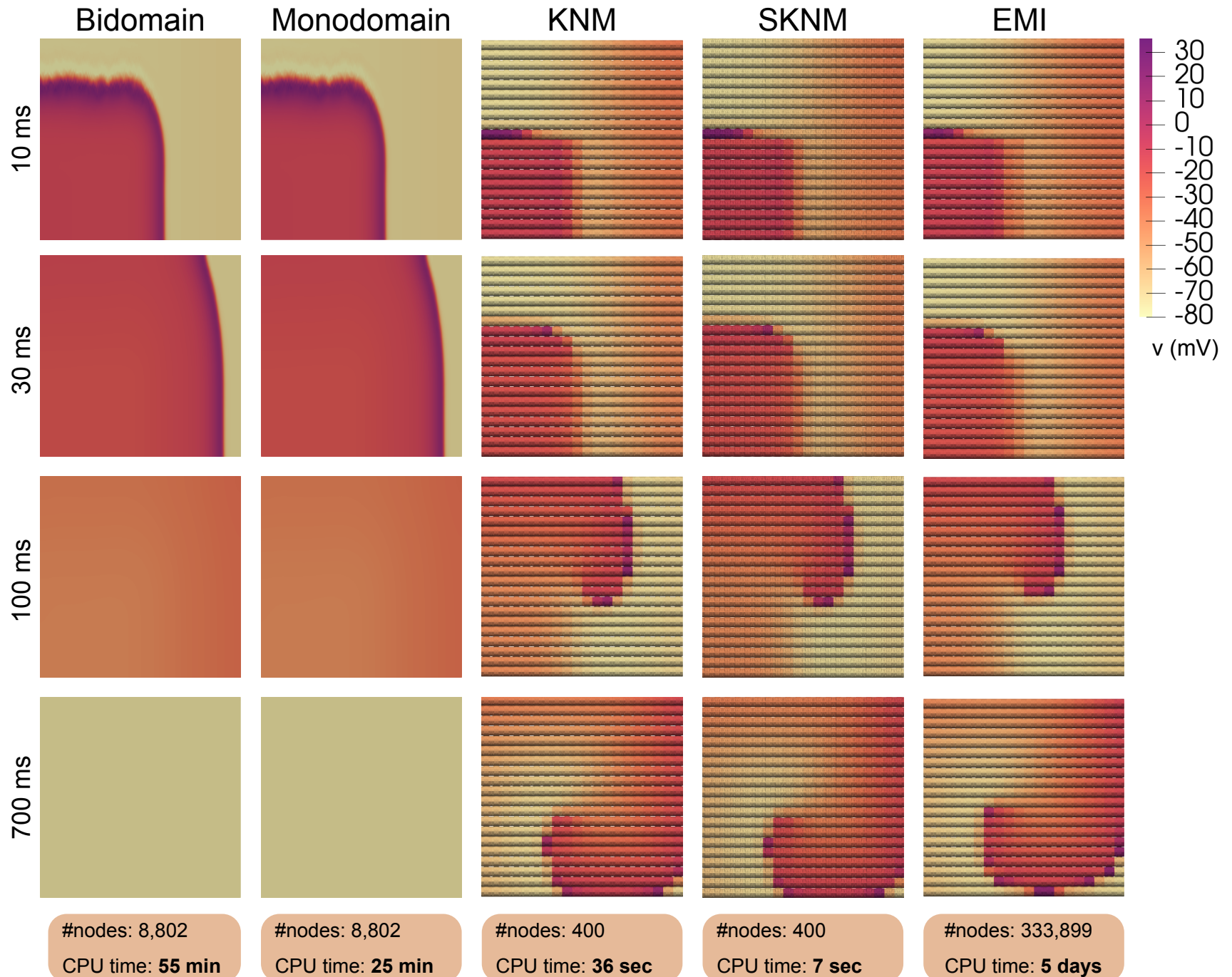


Model comparison: Micro reentry and CPU efforts

A spiral wave is generated for KNM, SKNM, and EMI, but not for the bidomain and monodomain models.

The simulations contain 20x20 weakly coupled cells, and an S2 stimulation is applied 240 ms after an S1 stimulation.

The CPU time required for each model simulation is reported in the lower panel.



Another example:

CPU time for simulating 50,625 hiPSC-CMs
(human induced pluripotent stem cell-derived cardiomyocytes,
immature cardiomyocytes)

Simulation time	10 ms	500 ms
Bidomain model	24,214 s	14 days
Monodomain model	470 s	6.5 h
Kirchhoff Network Model (KNM)	439 s	6.1 h
Simplified Kirchhoff Network Model (SKNM)	5.3 s	4.4 min

Averaging and homogenization are essential ways of dealing with the problem of different scales in biology.

In 1984, it was estimated that it would take 3000 years to solve the bidomain model for 10 ms using a mesh with a million nodes.

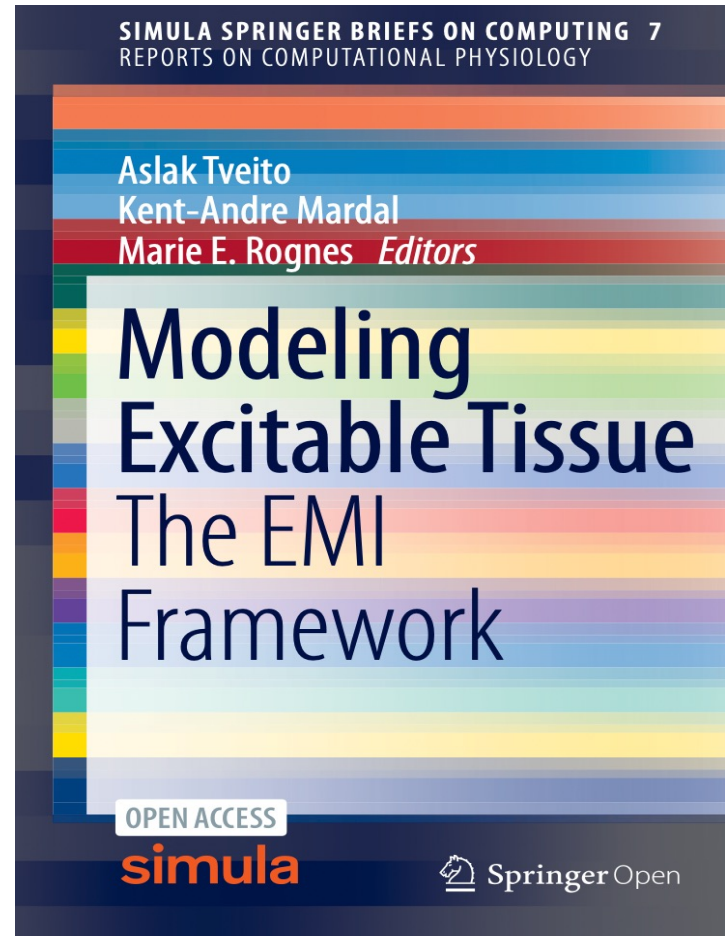
Today, bidomain and monodomain simulations are performed routinely.

Computers are now sufficiently powerful to allow for cell-level accuracy.

If you want the slides, please contact me at

aslak@simula.no

Thank you!



- [1] Reiss, Krzysztof, et al. "Overexpression of insulin-like growth factor-1 in the heart is coupled with myocyte proliferation in transgenic mice." *Proceedings of the National Academy of Sciences* 93.16 (1996): 8630-8635.
- [2] Doevedans, Pieter A., et al. "Cardiovascular phenotyping in mice." *Cardiovascular research* 39.1 (1998): 34-49.
- [3] Niederer, Steven, et al. "Simulating human cardiac electrophysiology on clinical time-scales." *Frontiers in physiology* 2 (2011): 14.
- [4] Niederer, Steven A., et al. "Verification of cardiac tissue electrophysiology simulators using an N-version benchmark." *Philosophical Transactions of the Royal Society A: Mathematical, Physical and Engineering Sciences* 369.1954 (2011): 4331-4351.
- [5] Clayton, R. H., and A. V. Panfilov. "A guide to modelling cardiac electrical activity in anatomically detailed ventricles." *Progress in biophysics and molecular biology* 96.1-3 (2008): 19-43.
- [6] Xie, Fagen, et al. "A simulation study of the effects of cardiac anatomy in ventricular fibrillation." *The Journal of clinical investigation* 113.5 (2004): 686-693.
- [7] <https://bionumbers.hms.harvard.edu/bionumber.aspx?id=110245&ver=3>
- [8] Barr RC, Plonsey R (1984) Propagation of excitation in idealized anisotropic two-dimensional tissue. *Biophysical Journal* 45(6):1191–1202

Simula publications on EMI

An Evaluation of the Accuracy of Classical Models for Computing the Membrane Potential and Extracellular Potential for Neurons

Aslak Tveito^{1,2*}, Karoline H. Jæger¹, Glenn T. Lines¹, Łukasz Paszkowski³, Joakim Sundnes^{1,2}, Andrew G. Edwards^{1,4}, Tuomo Mäki-Marttunen⁵, Geir Halnes⁶ and Gaute T. Einevoll^{6,7}

<https://doi.org/10.3389/fncom.2017.00027>

A Cell-Based Framework for Numerical Modeling of Electrical Conduction in Cardiac Tissue

Aslak Tveito^{1,2*}, Karoline H. Jæger¹, Miroslav Kuchta^{1,3}, Kent-Andre Mardal^{1,3} and Marie E. Rognes¹

<https://doi.org/10.3389/fphy.2017.00048>

How does the presence of neural probes affect extracellular potentials?

Alessio Paolo Buccino^{1,2} , Miroslav Kuchta³ , Karoline Horgmo Jæger⁴ , Torbjørn Vefferstad Ness^{1,5} , Pierre Berthet¹ , Kent-Andre Mardal^{3,4} , Gert Cauwenberghs²  and Aslak Tveito⁴ 

<https://doi.org/10.1088/1741-2552/ab03a1>

Properties of cardiac conduction in a cell-based computational model

Karoline Horgmo Jæger¹ , Andrew G. Edwards¹, Andrew McCulloch², Aslak Tveito^{1*}

<https://doi.org/10.1371/journal.pcbi.1007042>

Finite Element Simulation of Ionic Electrodiffusion in Cellular Geometries

Ada J. Ellingsrud^{1†}, Andreas Solbrå^{2,3†}, Gaute T. Einevoll^{2,3,4}, Geir Halnes^{2,4†} and Marie E. Rognes^{1*}

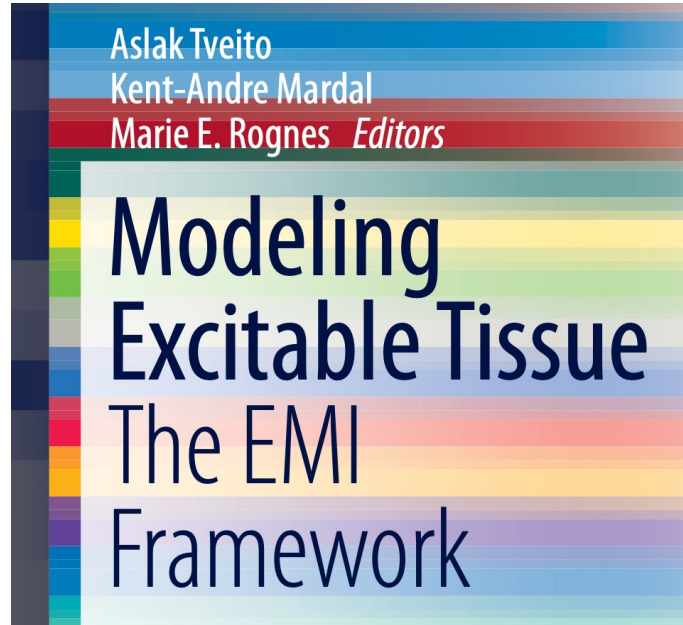
<https://doi.org/10.3389/fninf.2020.00011>

A computational method for identifying an optimal combination of existing drugs to repair the action potentials of SQT1 ventricular myocytes

Karoline Horgmo Jæger^{1*} , Andrew G. Edwards^{1,2} , Wayne R. Giles^{1,3}, Aslak Tveito¹ 

<https://doi.org/10.1371/journal.pcbi.1009233>

Simula publications on EMI



<https://doi.org/10.1007/978-3-030-61157-6>

Efficient Numerical Solution of the EMI Model Representing the Extracellular Space (E), Cell Membrane (M) and Intracellular Space (I) of a Collection of Cardiac Cells

Karoline Horgmo Jæger^{1*}, Kristian Gregorius Hustad¹, Xing Cai^{1,2} and Aslak Tveito^{1,2}

<https://doi.org/10.3389/fphy.2020.579461>

From Millimeters to Micrometers; Re-introducing Myocytes in Models of Cardiac Electrophysiology

Karoline Horgmo Jæger^{1*}, Andrew G. Edwards¹, Wayne R. Giles^{1,2} and Aslak Tveito¹

<https://doi.org/10.3389/fphys.2021.763584>

Deriving the Bidomain Model of Cardiac Electrophysiology From a Cell-Based Model; Properties and Comparisons

Karoline Horgmo Jæger^{1*} and Aslak Tveito^{1,2}

<https://doi.org/10.3389/fphys.2021.811029>

Arrhythmogenic influence of mutations in a myocyte-based computational model of the pulmonary vein sleeve

Karoline Horgmo Jæger¹, Andrew G. Edwards¹, Wayne R. Giles^{1,2} & Aslak Tveito¹

<https://doi.org/10.1038/s41598-022-11110-1>